Automotive Innovation (2024) 7:644–657
https://doi.org/10.1007/s42154-024-00288-x

Uncertainty Evaluation for Autonomous Vehicles: A Case Study of AEB System

Shunchang Duan[1,2,3] · Xianxu Bai[1,2,3] · Qin Shi[1,2] · Weihan Li[1,2,3] · Anding Zhu[3]

Received: 8 May 2023 / Accepted: 18 January 2024 / Published online: 28 October 2024

Abstract

To improve the safety of the intended functionality (SOTIF) performance of autonomous driving systems, this paper proposed a design method for autonomous driving systems with uncertainties. The automatic emergency braking (AEB) system is taken as an example to demonstrate the methodology. Firstly, uncertainty parameters in the AEB system model of typical working scenarios are defined and quantified, and a stochastic model of the AEB system with uncertainty parameters is established. Subsequently, the Monte Carlo simulation is employed to ascertain the actual safety distance distribution characteristics of the AEB system with uncertainties. The variance and width of the actual safety distance distribution are taken as response values to measure the reliability and robustness of the AEB system. The Box–Behnken design method is employed to design the uncertainty combination simulation test schemes. The surrogate models of uncertainty parameters with response variance and distributed width are established respectively, and the significance analyses are conducted. Finally, based on the variance surrogate models, the impact of uncertainties on the AEB system reliability and robustness is analyzed. This analysis provides the basis for the design of AEB system sensors. Based on the distributed width surrogate model, a dynamic safety distance adjustment mechanism is established to adjust the theoretical safety distance according to different uncertainties, thereby improving the reliability and robustness of the AEB system with multiple uncertainties. The method proposed in this paper provides a new idea for solving the SOTIF problems for autonomous driving systems.

Keywords Autonomous driving · SOTIF · Uncertainty · AEB · Statistical distribution

Abbreviations

AEB	Automatic emergency braking
BBD	Box–Behnken design
MCS	Monte Carlo simulation
MFDD	Mean fully developed deceleration
RSM	Response surface methodology
SOTIF	Safety of the intended functionality

1 Introduction

The safety of the intended functionality (SOTIF) problem is the crux of the long-tail effect in the application of autonomous driving technology [1]. A significant proportion of the research into the autonomous driving will focus on the SOTIF problems to improve the "last mile" technology. SOTIF concerns the system failing to achieve the intended function due to insufficient system functions, sensors or system impaired performances. Reasonably predictable misuse of personnel seriously threatens the safety of the autonomous driving system and becomes the biggest obstacle to the application of autonomous driving technology.

The lack of epistemic knowledge, the limitation of perceptual technology, and the deficiency of control accuracy in the design of the autonomous driving system, as well as the changes in the objective scenarios, may cause the performance indicators of the autonomous driving system to vary during the working process, resulting in the occurrence of SOTIF problems. Taking an autonomous driving system as an example, the National Highway Traffic Safety

✉ Xianxu Bai
bai@hfut.edu.cn

[1] Key Laboratory for Automated Vehicle Safety Technology of Anhui Province, Hefei University of Technology, Hefei 230009, China

[2] Engineering Research Center for Intelligent Transportation and Cooperative Vehicle-Infrastructure of Anhui Province, Hefei University of Technology, Hefei 230009, China

[3] Laboratory for Adaptive Structures and Intelligent Systems (LASIS), Department of Vehicle Engineering, Hefei University of Technology, Hefei 230009, China

Administration of the United States (NHTSA) announced three collisions with white trucks. All the accidents were caused by the perception system that recognized the white car as the sky under specific lighting conditions [2]. The impact of uncertainty factors faced by the system is beyond the expected range. In addition, in complex, chaotic, invisible, and highly uncertain scenarios [3] or severe weather conditions [4], the autonomous driving system often presents wrong or unexpected behaviors, leading to disastrous consequences. To mitigate the risk of SOTIF in autonomous driving, a comprehensive consideration of all kinds of uncertainties is essential for the system design. Through the strategic design and optimization of the scheme, the sensitivity of system performance to the impact of uncertainties and the risk of accidents under the impact of uncertainties are reduced in the pursuit of one or more optimal performances. It is of great significance to promote the application of the autonomous driving system.

In recent years, the rapid development of system design based on uncertainties and related uncertainty methods has provided solutions to improve the reliability and robustness of complex systems. Furthermore, its application in the field of vehicle design has also attracted extensive attention. A measure for the robustness of decision functions used in active safety systems for deciding on interventions to sensor measurement errors is introduced in Ref. [5]. Based on Monte Carlo simulations (MCS), Tobias et al. [6] investigates the effect of sensor measurement errors on the uncertainty of collision warning criteria used in collision warning systems. Shizhe et al. [7] analyzes their influence on the accuracy of predicted collision parameters like the time-to-collision (TTC) used in predictive passive safety systems. Uncertainty is introduced into the modeling of vehicle dynamics systems in Ref. [8] and proved that introducing uncertainty can significantly improve the model prediction accuracy and system robustness. An efficient uncertainty quantization method based on the definition, propagation, and verification of uncertainty is proposed in Ref. [9] to construct a dynamic model and a surrogate model for the vehicle. MCS is taken to verify the efficiency and accuracy of the model. Jan et al. [10] derived the collision probability model of the AEB system including sensor measurement error. It provided basis for the sensor selection of the AEB system. Christoph et al. [11–14] proposed a robust design method for AEB system considering sensor errors. The method was modified and applied to an automatic emergency steering system in Ref. [15].

Taking the AEB system as an example, this study introduces a design and optimization method of autonomous driving systems with uncertainties. As a pivotal component of the autonomous driving system, the robustness and reliability of the AEB system are inextricably linked to the safety of autonomous vehicles [16]. The robustness and reliability of the AEB system are inevitably affected by variable factors, such as limited sensor technology, scanty epistemic knowledge, and changeable working scenarios, which may lead to some SOTIF problems or even collisions [17]. In this work, the design method for autonomous driving systems with uncertainties is proposed, and the AEB system is taken as an example. The specific contributions are as follows:

(1) It is proposed to introduce parameter uncertainty of the automatic driving system, model and describe the uncertainty factors in the automatic driving system from the perspective of statistics. Furthermore, the existing vehicle kinematics and dynamics models is introduced to establish the system stochastic model with the introduction of uncertainty. The response model of the automatic driving system with uncertainty is constructed based on the stochastic model. The key parameters of the automatic driving system are specially designed and optimized, which provides a novel approach to enhance the adaptability of the automatic driving system and address the SOTIF problem.
(2) The AEB system is taken as an example. Uncertainties in the AEB system model under the typical working scenario are defined and quantified, and a stochastic model of the AEB system with uncertainties is established. The variance and width of the safety distance distribution under continuous multiple simulations by MCS are employed as the system response values. The surrogate models describing uncertainty parameters with response variance and distribution width are established, which provides an example for the design of the autonomous driving system with uncertainty.
(3) Based on the variance surrogate model, the sensitivity of each uncertainty parameter to the system response is analyzed, and the main parameters affecting system performance are found. The influence of main uncertainty parameter combinations on the system performance is evaluated through potentiometric maps, and the uncertainty parameter combination with the smallest variance is found. Based on the distributed width surrogate model, a dynamic safety distance adjustment mechanism is established, which can adjust the theoretical safety distance of the AEB system in real time according to the uncertainty of the current scenario, thus ensuring the reliability of the AEB system.

The paper is organized as follows. Section 2 describes the design method for autonomous driving systems with uncertainties. In Sect. 3, uncertainty parameters in the AEB

system model of typical working scenarios are defined and quantified, and a stochastic model of the AEB system with uncertainty parameters is established. Section 4 presents the surrogate models of uncertainty parameters with response variance and distributed width, respectively, and the significance analyses are conducted. In Sect. 5, based on the variance surrogate models, the impact of uncertainties on the AEB system reliability and robustness is analyzed. Based on the distributed width surrogate model, a dynamic safety distance adjustment mechanism is established to adjust the theoretical safety distance according to different uncertainties. Finally, Sect. 6 presents the conclusions.

2 Design Method for Autonomous Driving Systems with Uncertainties

The SOTIF problem represents one of the most significant challenges to the implementation of autonomous driving technology. The fundamental sources of SOTIF problems in autonomous driving are the uncertainties of elements in a scenario or parameters in an autonomous driving system. Therefore, the fundamental way to solve the SOTIF problems is to introduce the uncertainty of parameters in the design of an autonomous driving system, thereby improving its reliability and robustness of the autonomous driving system.

Figure 1 depicts the design method for the autonomous driving system with uncertainties. Firstly, the uncertainty system is modeled, including system modeling and uncertainty modeling. System modeling is the mathematical abstraction and expression of design and optimization problems. Generally, the modeling process for complex systems, such as vehicles, is gradually established on system-level, sub-system level, component level, and sub-system coupling models from macro to micro. The optimization variables, design space, system parameters, optimization objectives, and constraints at all levels are weighed and set reasonably. Subsequently, the multi-stage design and optimization models of the system are established. The objective of uncertainty modeling is to define and quantify the uncertainty factors involved in design and optimization, using appropriate uncertainty mathematical methods. Uncertainty is typically divided into two categories: aleatory uncertainty and epistemic uncertainty. Aleatory uncertainty refers to the inherent variability of the system and its working scenarios, such as perception error and solution error in the design of automatic driving systems. Epistemic uncertainty refers to the fact that designers cannot describe the actual value of some parameters or the exact probability distribution of uncertainty variables due to the lack of knowledge or information, such as modeling error, algorithm error, and simulation error. Secondly, the high-precision model analysis for the design of autonomous driving systems generally requires a large amount of calculation. If the uncertainty analysis and optimization are carried out directly based on the high-precision model, the calculation cost will be unbearable. An effective solution is to employ a data-driven approach to establish surrogate models, such as obtaining a large amount of test data through the MCS [18, 19] or profile tests to

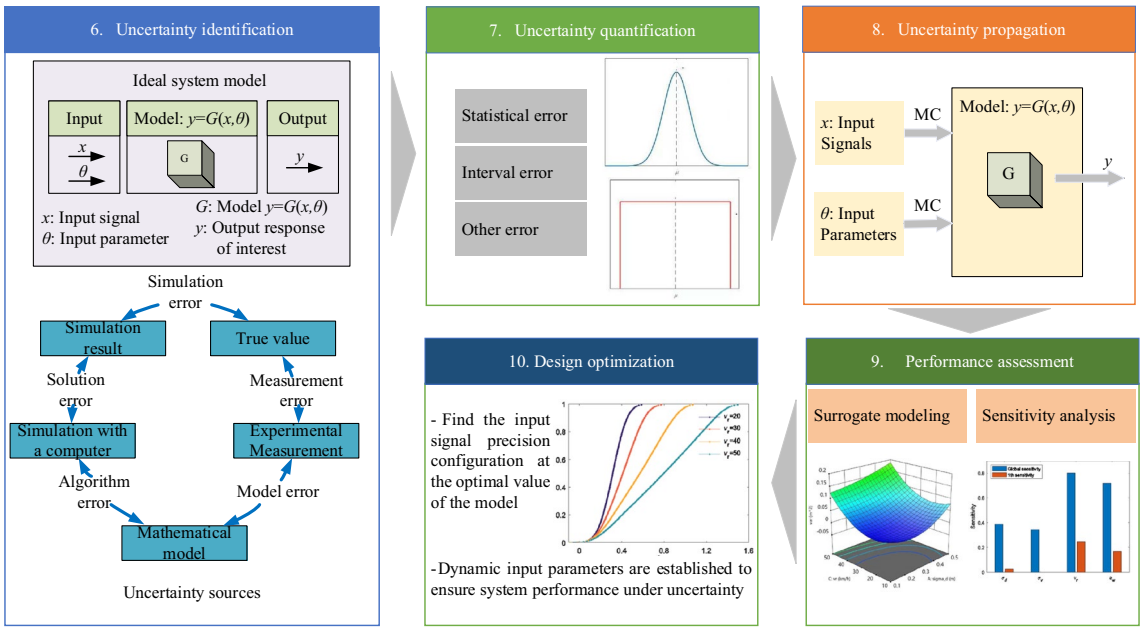

Fig. 1 The design method for autonomous driving systems with uncertainties

establish a surrogate model [20]. Then the surrogate models are used to replace the high-precision models for uncertainty analysis and optimization. In addition, due to the numerous uncertainty parameters involved in autonomous driving systems, the sensitivity analysis method is generally utilized to conduct significance analysis after the system uncertainty model is obtained. The parameters exhibiting weak impacts on system performance are filtered out to reduce the computational complexity of the design and optimization of the uncertainty system. Finally, uncertainty analysis is nested in system design and optimization. The distribution characteristics of system response under the impact of uncertainties are described. Meanwhile, the robustness and reliability of the design scheme are calculated. The objective is to identify the optimal scheme in the design space that meets the requirements of reliability and robustness.

The synergistic effect produced by the interaction and coupling of various components, which is fully considered in the design method for autonomous driving systems with uncertainties, is utilized to obtain the overall optimal solution of the system. The advantage of this method is to tap the design potential by considering the coupling between components. The scheme selection, evaluation, and optimization are carried out through a comprehensive analysis of the system. The method considers the uncertainty factors in the systems and their coupling influence adequately, which improves the robustness and reliability of the design scheme while pursuing the optimal performance of the autonomous driving systems. The method also helps to improve the overall design level of the autonomous driving system and provides a new idea to solve the SOTIF problems, which has bright application value and wide prospects.

3 Uncertainty Modeling of AEB System

3.1 AEB System Model Under the Typical Working Scenario

To illustrate the basic functions of the AEB system, a typical working scenario of the AEB system is shown in Fig. 2. Three vehicles are driving in the same lane and direction. The ego vehicle drives at a constant speed of v_{ego}, approaching a vehicle with a constant speed of v_{obj} at the distance d_r in front, and $v_{ego} > v_{obj}$. The relative distance between the two vehicles gradually decreases. To avoid the collision, the AEB system of the ego vehicle starts to brake until the two vehicles reach the same speed. Then, the relative distance between the two vehicles reaches the minimum value, which is denoted as the safety distance d_0. d_0 should be as small as possible to prevent the rear-end collision by the rear vehicle.

From the start of the AEB system, two vehicles reach the same speed, and the relationship of the driving distances between the two vehicles is:

$$L_{ego} = L_{obj} + d_r - d_0 \tag{1}$$

where L_{ego} is the distance passed by the ego vehicle, L_{obj} is the distance passed by the front vehicle, and d_r is the relative distance between two vehicles. Specifically,

$$L_{ego} = v_{ego} t_{ego} - \frac{1}{2} a_{ego} t_{ego}^2 \tag{2}$$

$$L_{obj} = v_{obj} t_{obj} \tag{3}$$

where t_{ego} is the time spent by the ego vehicle from the start of the AEB system to the two vehicles reaching the same speed. The time required by the AEB system, until the two vehicles reaching the same speed, is the time for the elimination of the relative speed of the two vehicles, which can be expressed as

$$t_{ego} = t_{obj} = \frac{v_r}{a_{ego}} \tag{4}$$

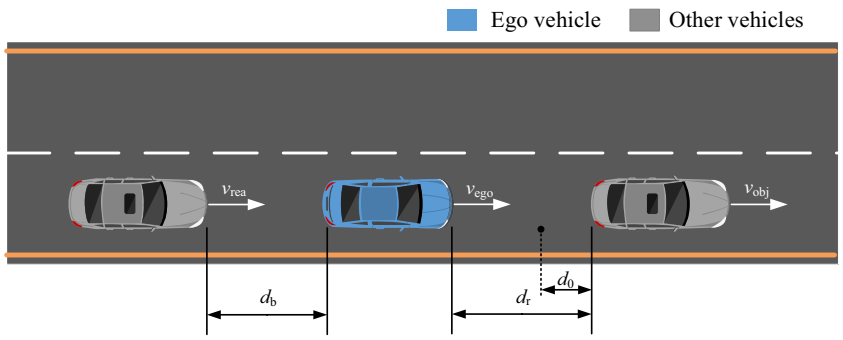

Fig. 2 A typical working scenario for the AEB system

where $v_r = v_{ego} - v_{obj}$. Assuming that the AEB system starts with full braking, the mean fully developed deceleration (MFDD) of the ego vehicle under the current working scenario is a_m, i.e., $a_{ego} = a_m$. After substituting Eqs. (2)–(4) into Eq. (1), the distance boundary d_{thr} of AEB system in the working scenario as shown in Fig. 1 is

$$d_{thr} = d_0 + \frac{v_r^2}{2a_m} \tag{5}$$

The theoretical safety distance d_0 when the two vehicles reach the same speed is

$$d_0 = d_{thr} - \frac{v_r^2}{2a_m} \tag{6}$$

where d_0 is a fixed value. d_0 should be as small as possible without collision with the vehicle in front, to improve road efficiency and avoid rear-end collision by the vehicle behind.

3.2 Stochastic Model of the AEB System with Uncertainty

According to the AEB system model under the typical working scenario, the parameters needed in the AEB system working scenario are divided into two types: deterministic parameters and uncertainty parameters. Deterministic parameters refer to a class of parameters in the model which are known or recognized and given definite values. The uncertainty parameters refer to a kind of parameter whose value cannot be obtained accurately or are distributed in statistical form. d_{thr} and v_r are acquired by millimeter-wave radars, lidars, or other sensors with stochastic noises, which are generally considered to follow the Gaussian distribution [21]. a_m is the MFDD of a vehicle in the braking process. The MFDD is related to road materials, road conditions, tire structure, tread pattern, materials, vehicle speed, control logic of anti-lock braking system, and other factors, which have extensive epistemic uncertainty and are expressed in the form of intervals [22]. The specific distribution forms are shown in Table 1.

As shown in Table 1, $\hat{d}_{thr}$, $\hat{v}_r$ and $\hat{a}_m$ are the uncertainty parameters in the AEB system model under the typical working scenario. d_{thr}, v_r and a_m are the standard true values of the corresponding uncertainty parameters. $N(d_{thr}, \sigma_d^2)$ indicates that $\hat{d}_{thr}$ is subject to a Gaussian distribution whose mathematical expectation is d_{thr}, and variance is σ_d^2. $N(v_r, \sigma_v^2)$ indicates that $\hat{v}_r$ is subject to a Gaussian distribution whose mathematical expectation is v_r, and variance is σ_v^2. a_m is usually estimated by employing tire dynamics, vision, or other methods. The estimation error is inevitable. Besides, a_m fluctuates under the impact of various variable factors in the braking process. The true value of a_m is assumed to be distributed within the symmetric interval $[a_m - a_w, a_m + a_w]$ with a width of $2a_w$. a_w is affected by tire and road conditions, weather, temperature, etc.

After introducing the uncertainty of parameters, the theoretical distance boundary d_{thr} of AEB system startup under a typical scenario is

$$d_{thr} = d_0 + \frac{\hat{v}_r^2}{2a_m} \tag{7}$$

The actual safety distance $\hat{d}_0$ when two vehicles reach the same speed is

Table 1 Uncertainty parameter Settings

Parameters	Truth value	Source	Types	Distribution	Ranges
$\hat{d}_{thr}$	d_{thr}	Sensor	Aleatory uncertainty	Gaussian	$N(d_{thr}, \sigma_d^2)$
$\hat{v}_r$	v_r	Sensor	Aleatory uncertainty	Gaussian	$N(v_r, \sigma_v^2)$
$\hat{a}_m$	a_m	Estimation	Epistemic uncertainty	Interval	$[a_m - a_w, a_m + a_w]$

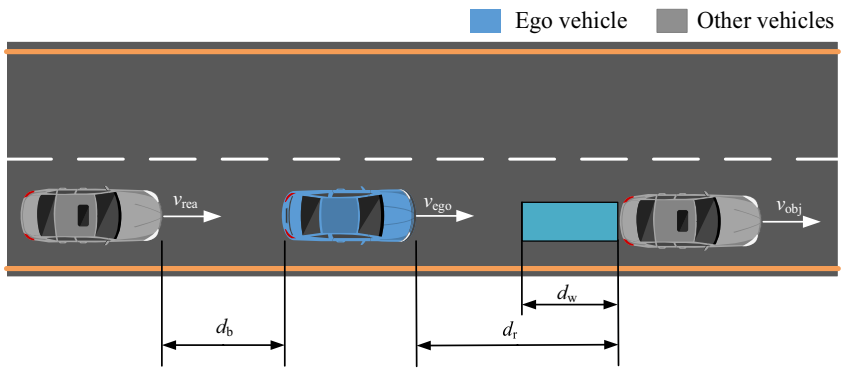

Fig. 3 AEB system model with uncertainty parameters

$$\hat{d}_0 = \hat{d}_{\text{thr}} - \frac{\hat{v}_{\text{r}}^2}{2\hat{a}_{\text{m}}} \tag{8}$$

where $\hat{d}_{\text{thr}}$ is subject to a Gaussian distribution of $N\left(d_{\text{thr}}, \sigma_d^2\right)$. Combing Eqs. (7) and (8), the stochastic model of the AEB system can be obtained. After introducing the uncertainty of parameters, the actual safety distance $\hat{d}_0$ is affected byσ_d, σ_v, v_{r} and a_{w}. As illustrated in Fig. 3, the actual safety distance $\hat{d}_0$ is distributed in the range of width d_{w}. To analyze the distribution characteristics of $\hat{d}_0$, a theoretical model of uncertainty parameters and the distribution characteristics of $\hat{d}_0$ should be established based on large amounts of simulation or experimental data. The major uncertainty parameters that affect the distribution characteristics of $\hat{d}_0$ should be analyzed. Thus, suggestions for the design and optimization of the AEB system can be provided.

4 Surrogate Model for Safety Distance Distribution of AEB System

4.1 Actual Safety Distance Distribution Statistics Based on MCS

As shown in the stochastic model of the AEB system with uncertainty, the distribution of the actual safety distance $\hat{d}_0$ of the AEB system is affected by parameters such as σ_d, σ_v, v_{r} and a_{w}. There are many uncertainty parameters and strong coupling. MCS can simulate real complex systems directly, which is suitable for solving high-dimensional, complex, and time-continuity problems. Its versatility renders it a valuable tool in a wide range of applications. Therefore, the MCS method was applied to the stochastic model of the AEB system to obtain the distribution characteristics of $\hat{d}_0$ in different combinations of uncertainty parameters within the error range. Figure 4 depicts the distribution of $\hat{d}_0$ under a special combination of σ_d, σ_v, v_{r} and a_{w} obtained by MCS.

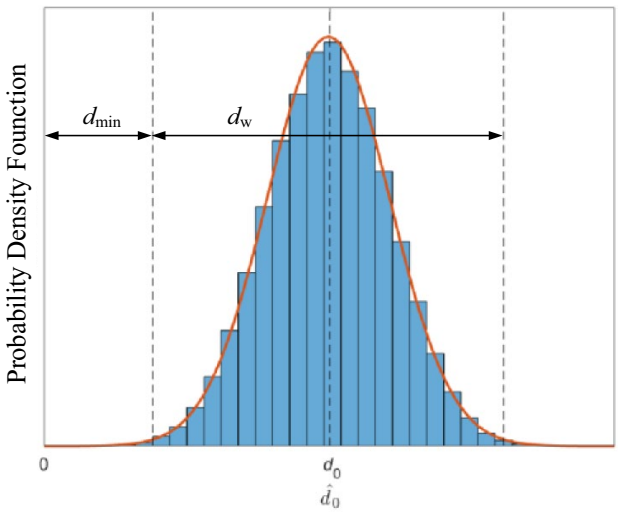

Fig. 4 Distribution diagram of $\hat{d}_0$ in a combination of uncertainty parameters

As shown in Fig. 4, the actual safety distance $\hat{d}_0$ is symmetrically distributed on both sides of the theoretical safety distance d_0. The farther away from the theoretical safety distance d_0, the lower the probability density. The variance (var) of the distribution of the actual distance $\hat{d}_0$ obtained by N times of MCS, that is, the average value of the square of the distance between d_0 and $\hat{d}_0$, is taken to describe the deviation between the actual and theoretical safety distance. The variance, var, is utilized as the evaluation index of the accuracy and reliability of the AEB system, which is expressed as

$$var = \frac{\sum_1^N (\hat{d}_0 - d_0)^2}{N} \tag{9}$$

where N is the sampling times of MCS (10^4 times in the study). The smaller the var, the lesser deviation between $\hat{d}_0$ and d_0, thereby increasing the accuracy and reliability of the AEB system. As shown in Fig. 4, the 99.7% concentrated distribution range of $\hat{d}_0$ is defined as the distribution width d_{w}, and $d_{\min}$ is the minimum relative distance between two vehicles when $\hat{d}_0$ is in the range of d_{w}.

4.2 Establishment of Surrogate Models and Significance Tests

Although the MCS can address the issue of system response with numerous uncertainty parameters, it is not suitable for the multi-level uncertainty of parameters. The surrogate model, based on experimental data, provides a feasible approach to solving the multi-level problem of uncertainty, which can be taken to replace the real response function after introducing multi-factors and multi-level uncertainty parameters.

Response Surface Methodology (RSM) [23] is a representative method of surrogate model technology [24]. RSM extracts certain sample points from the input parameters through a specific sampling method and carries out uncertainty tests or simulation analyses on these sample points to obtain the corresponding response sample points. Polynomial is typically employed to fit the sample data to generate a reliability analysis response surface model including uncertainty parameters. RSM is based on the sample data, which determines the prediction accuracy of the response surface model in the uncertainty parameters space. To construct a response surface model with high precision, a group of representative sample points should be reasonably selected to reflect the variation characteristics of uncertainty parameters space, while maintaining a limited sample point size. The Box–Behnken design (BBD) method [25] can control the selected sample points within the range of uncertainty

parameters uniformly. The method has the advantages of fewer test times, short cycles, and high accuracy. In the study, to obtain the RSM model of the minimum safe distance distribution variance and distribution width of the AEB system under typical scenarios, the BBD experimental design method was adopted to arrange the combinations of uncertainty parameters reasonably. The MCS method was taken to obtain the AEB system response value under each uncertain combination. In addition, to eliminate the difference of parameters in the variation range and order of magnitude, four uncertainty parameters, σ_d, σ_v, v_r, and a_w, introduced by the stochastic model of the AEB system are denoted as A, B, C, and D, respectively. Referring to the sensor accuracy level provided by Stöckle [13] and the research of Žuraulis [26] on vehicle MFDD, three levels are taken from each of the uncertainty parameters, as shown in Table 2.

Table 2 The uncertainty parameters coding with three levels

Parameters	Level		
	Low (−1)	Medium (0)	High (+1)
σ_d (A)	0.1	0.3	0.5
σ_v (B)	0.1	0.3	0.5
v_r (C)	10	30	50
a_w (D)	0.2	0.4	0.6

The simulation results for BBD with four parameters and three levels are shown in Table 3. For each scheme in the table, the MSC is taken to simulate, and the response value is recorded. There are 29 sample points in the scheme, of which 24 are factorial points and 5 zero points are taken for error estimation. Based on the simulation results in Table 3, multiple regression analyses on var and the var response surface model establishment are conducted using Design-Expert® software. The results can be expressed as follows:

Table 3 The simulation result for BBD with four parameters and three levels

Number	A		B		C		D		Response	
	Code value	Truth value	Code value	Truth value	Code value	Truth value	Code value	Truth value	var	d_w
1	0	0.3	0	0.3	0	30	0	0.4	0.0254	0.8254
2	0	0.3	−1	0.1	1	50	0	0.4	0.1406	1.5553
3	0	0.3	−1	0.1	0	30	−1	0.2	0.0124	0.6404
4	0	0.3	0	0.3	0	30	0	0.4	0.0253	0.8224
5	0	0.3	0	0.3	0	30	0	0.4	0.0253	0.8168
6	−1	0.1	1	0.5	0	30	0	0.4	0.0174	0.4991
7	0	0.3	0	0.3	−1	10	1	0.6	0.0087	0.5496
8	0	0.3	0	0.3	1	50	1	0.6	0.3071	2.1655
9	1	0.5	−1	0.1	0	30	0	0.4	0.0794	1.6457
10	−1	0.1	−1	0.1	0	30	0	0.4	0.0172	0.4771
11	1	0.5	0	0.3	0	30	−1	0.2	0.0669	1.5502
12	0	0.3	0	0.3	0	30	0	0.4	0.0253	0.8324
13	−1	0.1	0	0.3	0	30	1	0.6	0.0392	0.7068
14	1	0.5	0	0.3	1	50	0	0.4	0.1951	2.2890
15	0	0.3	1	0.5	−1	10	0	0.4	0.0084	0.5428
16	0	0.3	1	0.5	0	30	−1	0.2	0.0124	0.6442
17	−1	0.1	0	0.3	1	50	0	0.4	0.1319	1.2783
18	0	0.3	0	0.3	−1	10	−1	0.2	0.0081	0.5438
19	1	0.5	0	0.3	−1	10	0	0.4	0.0625	1.4871
20	0	0.3	−1	0.1	0	30	1	0.6	0.0467	1.0232
21	−1	0.1	0	0.3	−1	10	0	0.4	0.0003	0.0919
22	0	0.3	−1	0.1	−1	10	0	0.4	0.0083	0.5433
23	1	0.5	0	0.3	0	30	1	0.6	0.1011	1.8056
24	0	0.3	0	0.3	1	50	−1	0.2	0.0412	0.9786
25	0	0.3	1	0.5	0	30	1	0.6	0.0471	1.0325
26	0	0.3	1	0.5	1	50	0	0.4	0.1417	1.5672
27	0	0.3	0	0.3	0	30	0	0.4	0.0254	0.8233
28	1	0.5	1	0.5	0	30	0	0.4	0.0795	0.9962
29	−1	0.1	0	0.3	0	30	−1	0.2	0.0044	0.2563

$$\begin{aligned}\mathrm{var} &= 0.0253 + 0.0311A + 0.0001B + 0.0829C + 0.0666D \\ &\quad + 0.0003AC - 0.0001AD + 0.0002BC + 0.0001BD + 0.0663CD \\ &\quad + 0.021A^2 - 0.002B^2 + 0.0533C^2 + 0.0085D^2 - 0.0168A^2C \\ &\quad - 0.0494A^2D + 0.0002AC^2 - 0.0165B^2C - 0.0494B^2D + 0.0002BC^2\end{aligned} \tag{10}$$

Regression analysis of variance and significance test is performed on the regression equation, and the results are listed in Table 4. According to Table 4, $F = 179.64 \geq F_{0.01}(20, 6) = 7.40$, $p < 0.0001$, indicating that the regression equation is extremely significant. The determination coefficient $R^2 = 0.9985$, indicating that the equation can well reflect the relationship between the uncertainty parameters, that is, σ_d, σ_v, v_r, a_w, and the response value (variance var). The adjustment coefficient R^2_{adj}=0.9929, indicating that the regression equation can explain 99.29% of the response value changes, and the signal-to-noise ratio (resolution) of the model is 58.2721, larger than 4, indicating that the model has enough resolution. The polynomial obtained is feasible as a surrogate model of the real model response.

Similarly, based on the simulation results in Table 3, multiple regression analysis is conducted on distribution width d_w to establish the response surface model of d_w. The results can be expressed as follows:

$$\begin{aligned}d_w &= 0.8241 + 0.5982A + 0.0033B + 0.5127C \\ &\quad + 0.2982D - 0.1679AB - 0.0961AC \\ &\quad - 0.0488AD + 0.0031BC + 0.0014BD \\ &\quad + 0.2953CD + 0.1871A^2 - 0.0524B^2 \\ &\quad + 0.2508C^2 + 0.0388D^2 - 0.1602A^2B \\ &\quad - 0.0156A^2C - 0.1217A^2D - 0.1818AB^2 \\ &\quad + 0.0033AC^2 - 0.0036B^2C \\ &\quad - 0.1054B^2D - 0.0004BC^2\end{aligned} \tag{11}$$

The variance analysis and significance test results for d_w regression equations are listed in Table 5. According to Table 5, $F = 65.33 \geq F_{0.01}(20,6) = 7.40$, $p < 0.0001$, indicating that the regression equation is extremely significant. The determination coefficient $R^2 = 0.9958$, indicating that the equation can well reflect the relationship between the uncertainty parameters, i.e., σ_d, σ_v, v_r, a_w, and the response value (distribution width d_w). The adjustment coefficient R^2_{adj}=0.9806, indicating that the regression equation can explain 98.06% of the response value changes, and the signal-to-noise ratio (resolution) of the

Table 4 Variance analysis and significance test for var regression equations

Source	Sum of squares	Degree of freedom	Mean square	*F* value	Prob > *F*
Model	0.1325	22	0.0060	179.64	< 0.0001
A	0.0039	1	0.0039	115.36	< 0.0001
B	4.000×10^{-8}	1	4.000×10^{-8}	0.0012	0.9736
C	0.0275	1	0.0275	819.21	< 0.0001
D	0.0178	1	0.0178	529.45	< 0.0001
AB	2.500×10^{-9}	1	2.500×10^{-9}	0.0001	0.9934
AC	2.500×10^{-7}	1	2.500×10^{-7}	0.0075	0.9340
AD	9.000×10^{-8}	1	9.000×10^{-8}	0.0027	0.9604
BC	2.500×10^{-7}	1	2.500×10^{-7}	0.0075	0.9340
BD	4.000×10^{-8}	1	4.000×10^{-8}	0.0012	0.9736
CD	0.0176	1	0.0176	524.69	< 0.0001
A^2	0.0028	1	0.0028	84.97	< 0.0001
B^2	0.0000	1	0.0000	0.7860	0.4094
C^2	0.0185	1	0.0185	550.19	< 0.0001
D^2	0.0005	1	0.0005	14.00	0.0096
A^2B	1.250×10^{-9}	1	1.250×10^{-9}	0.0000	0.9953
A^2C	0.0006	1	0.0006	16.88	0.0063
A^2D	0.0049	1	0.0049	145.39	< 0.0001
AB^2	1.250×10^{-9}	1	1.250×10^{-9}	0.0000	0.9953
AC^2	1.250×10^{-7}	1	1.250×10^{-7}	0.0037	0.9533
B^2C	0.0005	1	0.0005	16.19	0.0069
B^2D	0.0049	1	0.0049	145.39	< 0.0001
BC^2	8.000×10^{-8}	1	8.000×10^{-8}	0.0024	0.9626
Residual	0.0002	6	0.0000	$R^2 = 0.9985$	$R^2_{adj} = 0.9929$
Total	0.1327	28	Adeq precision = 58.2721		

Table 5 Variance analysis and significance test for d_w regression equations

Source	Sum of squares	Degree of freedom	Mean square	F value	Prob > F
Model	8.53	22	0.3876	65.33	< 0.0001
A	1.43	1	1.43	241.24	< 0.0001
B	0.0000	1	0.0000	0.0072	0.9350
C	1.05	1	1.05	177.20	< 0.0001
D	0.3556	1	0.3556	59.94	0.0002
AB	0.1127	1	0.1127	19.00	0.0048
AC	0.0370	1	0.0370	6.23	0.0468
AD	0.0095	1	0.0095	1.60	0.2523
BC	0.0000	1	0.0000	0.0065	0.9385
BD	7.562×10^{-6}	1	7.562×10^{-6}	0.0013	0.9727
CD	0.3487	1	0.3487	58.78	0.0003
A^2	0.2272	1	0.2272	38.29	0.0008
B^2	0.0178	1	0.0178	3.00	0.1339
C^2	0.4079	1	0.4079	68.76	0.0002
D^2	0.0098	1	0.0098	1.65	0.2466
A^2B	0.0513	1	0.0513	8.65	0.0259
A^2C	0.0005	1	0.0005	0.0820	0.7842
A^2D	0.0296	1	0.0296	4.99	0.0669
AB^2	0.0661	1	0.0661	11.14	0.0157
AC^2	0.0000	1	0.0000	0.0037	0.9537
B^2C	0.0000	1	0.0000	0.0043	0.9498
B^2D	0.0222	1	0.0222	3.74	0.1011
BC^2	3.612×10^{-7}	1	3.612×10^{-7}	0.0001	0.9940
Residual	0.0356	6	0.0059	$R^2=0.9958$	$R^2_{adj}=0.9806$
Total	8.56	28	Adeq precision = 32.0295		

model is 32.0295, which is larger than 4, indicating that the model has enough resolution. The polynomial obtained is feasible as a surrogate model of the real model response.

5 Design and Optimization of AEB System with Parameter Uncertainty

The surrogate models accurately describe the relationship between parameter uncertainties with variance var and width d_w in the AEB system. Var represents the deviation degree between the actual safety distance $\widehat{d}_0$ and the theoretical safety distance d_0 of the AEB system. The smaller the variance, the smaller the deviation degree between d_0 and $\widehat{d}_0$, and the better the stability of the AEB system. To reasonably configure the uncertainty of each parameter and maintain var at a low level, it is necessary to design the uncertainty range of each parameter. Firstly, based on the var surrogate model, the sensitivity of each uncertain parameter to the system response is analyzed, and the main parameters affecting variance are found. Then, the influence of main uncertainty parameter combinations on the system performance is analyzed by potentiometric maps, and the uncertainty parameter combination with the smallest variance is found. Since the uncertainty of each parameter cannot be eliminated in the actual situation, to ensure vehicles' safety under the uncertainty parameters, a dynamic safety distance adjustment mechanism is established based on the d_w surrogate model to optimize the system. The dynamic safety distance adjustment mechanism can adjust the theoretical safety distance in real time according to the current uncertainties, thereby ensuring the reliability of the AEB system.

5.1 Sensitivity Analysis of Uncertainty Parameters

Var is affected by numerous parameters, including σ_d, σ_v, v_r and a_w. Among them, σ_d and σ_v are mainly limited by the technical level and cost of sensors. v_r is closely related to the working scenarios of the AEB system. a_w is limited by the current cognition of the interaction between tires and road surface, which is typically at a fixed level. To reduce the level of var and improve the reliability of the AEB system, the impact of various uncertainty parameters on var should be compared firstly. The impact of parameter variation on

model response can be analyzed by Sobol' sensitivity analysis method [27], which calculates the impact of parameters' which sample variance on the total variance of model response. Therefore, the Sobol' method is taken to analyze the sensitivity of parameters σ_d, σ_v, v_r and a_w. Moreover, the calculation results of Sobol' method have a large relationship with the sample size, making it challenging to accurately assess the real impact of parameter variation on the model response when the sample size is limited. In the study, the sample size was set to 10^4 and 10^5 times, respectively. The histogram was drawn according to the sensitivity of each parameter to var, as shown in Fig. 5(a), (b).

According to Fig. 5(a), (b), the results of the two sensitivity analyses are consistent, suggesting that the sensitivity analysis data at the sample scale of 10^4 has reached stability and that the results of the sensitivity analysis are reliable. Sensitivity analysis data shows that, within the range of uncertainty parameters values, parameter v_r has the most significant effect on var, parameter σ_d and a_w have a certain effect on var, and parameter σ_v has a very weak effect on var. The global sensitivity is greater than the first-order sensitivity, indicating that the interaction of parameters has a

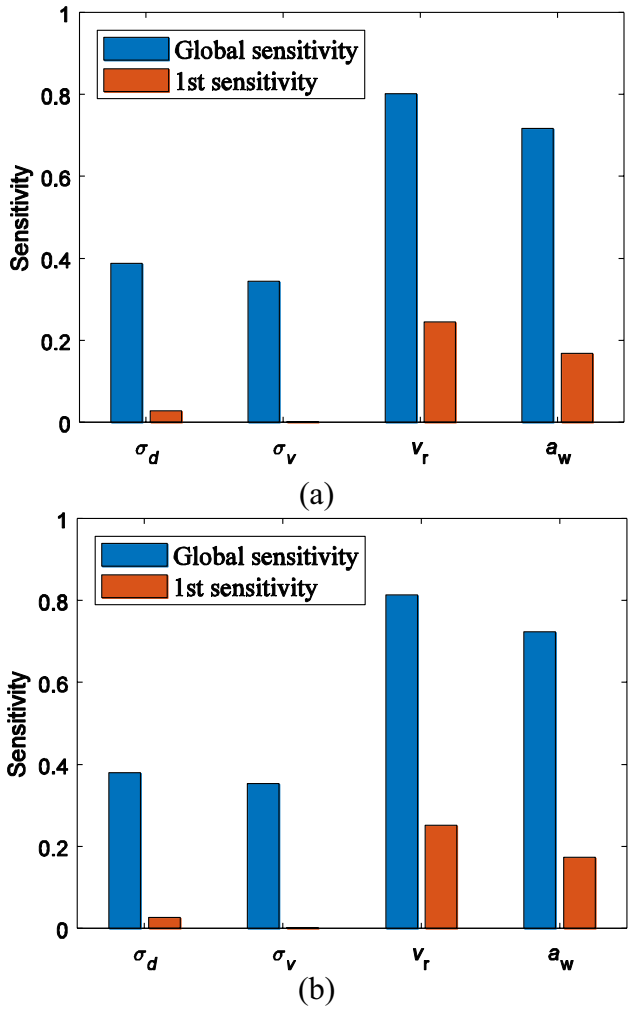

Fig. 5 Sobol' sensitivity analysis results

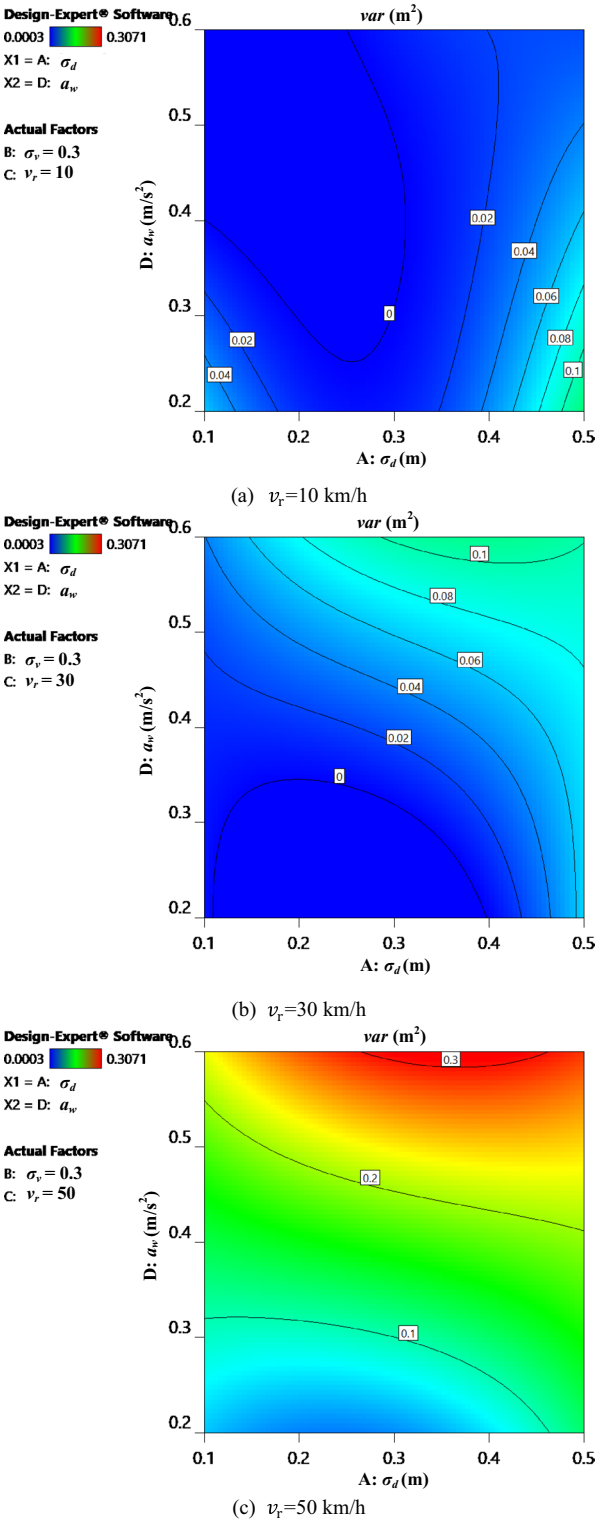

Fig. 6 Potentiometric maps of var at different v_r

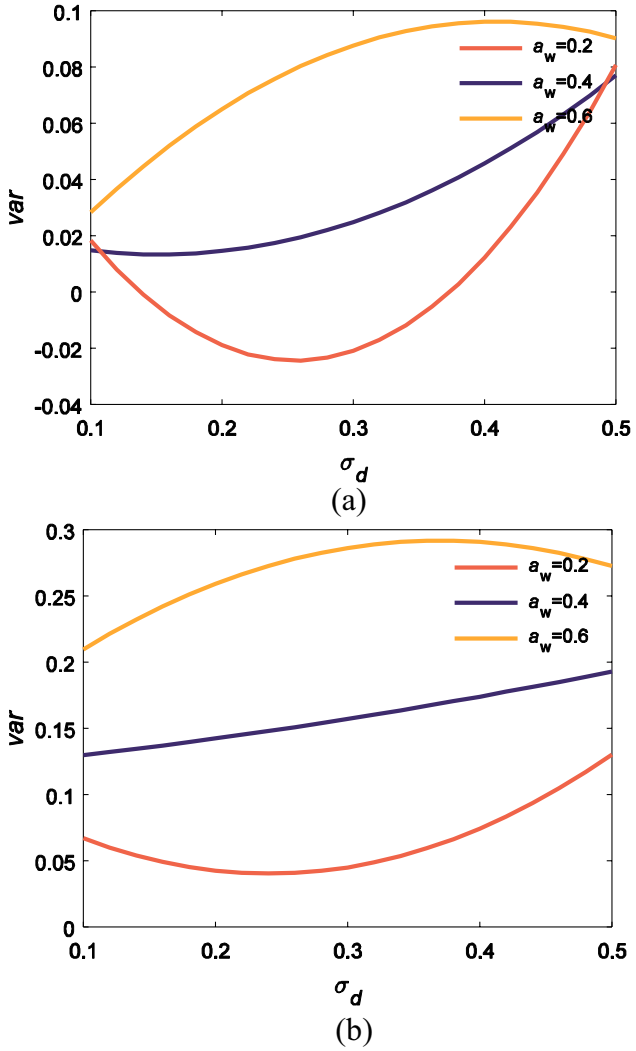

Fig. 7 The interaction between σ_d and a_w at different v_r

significant effect on var. Based on the above analysis, the main parameter affecting var is the relative speed v_r, which is related to AEB system working scenarios. Subsequently, it is necessary to match the appropriate safety distance d_0 for different working scenarios to improve the reliability of the AEB system. In the scenario when v_r is fixed, the impact of the interactions between σ_d and a_w on var should be considered specially. Moreover, due to the limitation of the epistemic uncertainty of a_w, the level of a_w cannot be improved in the short term. In the design of the AEB system, due to the interaction between σ_d and a_w, unilateral enhancement of σ_d may have a limited improvement on the reliability of the AEB system and increase the cost of the AEB system. Therefore, it should be considered to maintain the balance between the cost and the reliability in the design of the AEB system. In addition, since the σ_v has little effect on var within its value range, the sensor accuracy for distance should be considered especially when selecting millimeter-wave radar or lidar.

5.2 Parameter Design of AEB System's Sensor

Based on the sensitivity analysis of the var response surface model, the design goal of the AEB system is to find the optimal σ_d corresponding to a fixed a_w to minimize the var of actual safety distance distribution of the AEB system in various scenarios. Figure 6 shows the potentiometric maps of var under different v_r. Figure 6(a) illustrates the impact of the interactions between σ_d and a_w on var, when v_r = 10 km/h. In the majority of regions depicted in Fig. 6(a), the var is smaller than 0.02, indicating that the overall impact of σ_d and a_w on var is relatively insignificant. As v_r increases, var increases gradually, which indicates that the impact of the interactions between σ_d and a_w on var gradually increases, as shown in Fig. 6(b), (c). Figure 6(b), (c) depict the potentiometric maps when v_r = 30 km/h and 50 km/h, respectively. When v_r = 30 km/h, var increases with σ_d and a_w in a similar amplitude, which indicates that σ_d and a_w have a comparable impact on var when v_r = 30 km/h. When v_r = 50 km/h, the variation degree of var when a_w varies is greater than that when σ_d varies. To describe the interaction between σ_d and a_w more accurately, a_w is fixed at three levels, and the variations var with σ_d at each level are plotted in Fig. 7.

As shown in Fig. 7(a), (b), at the same a_w, var exhibits a consistent trend with an increase in σ_d. At the medium level (a_w=0.4), it conforms to the general cognition that the higher precision of the sensor system, the better the system performance. However, at the low level (a_w=0.2), var firstly decreases and then increases with an increase in σ_d, while at the high level (a_w=0.6), var firstly increases and then decreases with an increase in σ_d. This shows that improving σ_d unilaterally cannot guarantee the system's better performance. Figure 7(b) is taken as an example, when a_w is low, the system's performance at σ_d=0.25, which is at the lowest point of var, is better than that of σ_d=0.1. Compared with the increase in sensor cost caused by σ_d=0.1, σ_d=0.25 brings better performance and substantial cost savings. When a_w is high, the system performance is almost the same when σ_d is 0.5 and 0.25. Through the analysis of the uncertainty parameters for autonomous driving systems, it can not only optimize the system design and obtain the parameter configuration of the system to achieve the best performance, but also avoid the waste of resource allocation and achieve balance between performance and cost.

5.3 Dynamic Safety Distance Adjustment Mechanism of AEB System

The d_w response surface model provides a comprehensive analysis of the influence of uncertainty parameters on the

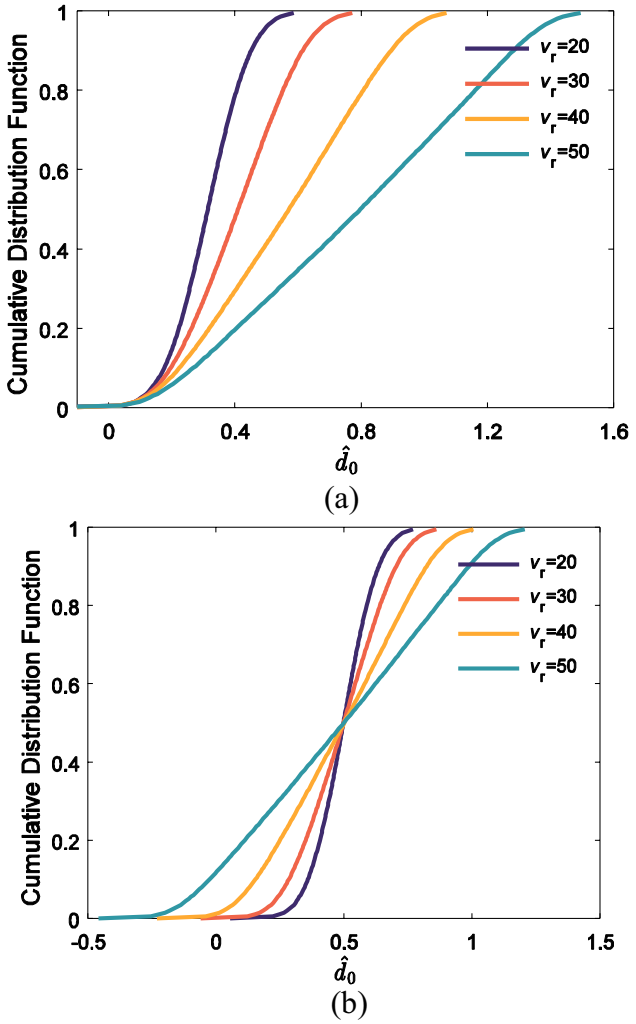

Fig. 8 The cumulative distribution function of $\hat{d}_0$ distribution under different relative speeds

distribution width of the safety distance d_0 for the AEB system. d_w of the AEB system varies according to the decrease in precision of sensors because of inclement weather or aging, as well as the changes in relative speed. Furthermore, the actual safety distance $\hat{d}_0$ is symmetrically distributed on both sides of the theoretical safety distance d_0. To make d_0 as small as possible without colliding with the vehicle in front, the theoretical safety distance d_0 should satisfy:

$$d_0 \geq \frac{d_w}{2} + s \tag{12}$$

where s is the safety margin. d_w is shown in Eq. (11). Equation (12) represents the dynamic safety distance adjustment mechanism, which is the minimum safety distance to avoid collision with the front vehicle.

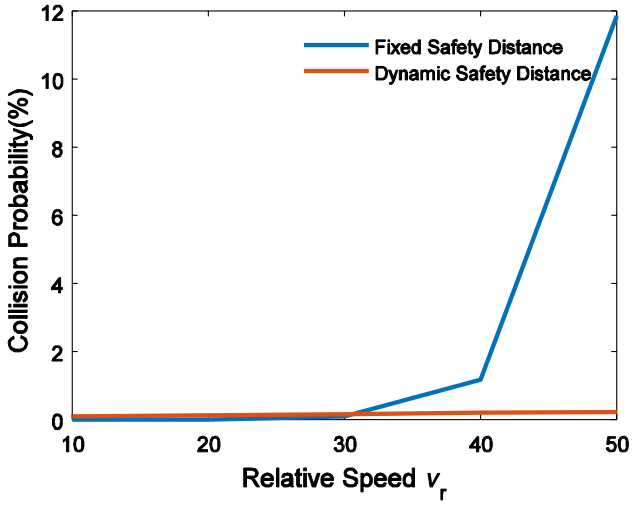

Fig. 9 Collision probability of two vehicles at different relative speeds

To verify the effectiveness of the dynamic safety distance adjustment mechanism, the simulation tests are carried out in the typical operation scenario of the AEB system shown in Fig. 2, the AEB system adopts the control strategy based on safety distance shown in Eq. (5). The sensor precision σ_d and σ_v of AEB system are set as 0.3, the current level of a_w is fixed at 0.4, and s is set as 0. Figure 8 shows the cumulative distribution function of the actual safety distance $\hat{d}_0$ of the AEB system under the dynamic safety distance adjustment mechanism when v_r is between 20 km/h to 50 km/h and d_0 is fixed at 0.5 m. As shown in Fig. 8(a), (b), for the two types of strategies at a v_r, the widths of the distributions of $\hat{d}_0$ are the same. The difference is that, as shown in Fig. 8(a), the probabilities of $\hat{d}_0 = 0$ under different v_r are 0, which means that there will be no collision between the two vehicles at any v_r. But in Fig. 8(b), the probability of $\hat{d}_0 = 0$ increases as v_r increases. As a result, the vehicle has a large collision probability at a large v_r.

Figure 9 shows the change in collision probability of two vehicles with the change of relative speed under the two strategies of dynamic safety distance adjustment mechanism and the fixed safety distance, respectively. As illustrated in Fig. 9, if the fixed safety distance is adopted, the collision probability of two vehicles increases gradually with the increase of v_r, when the v_r reaches 50 km/h, and the collision probability of two vehicles reaches 12%. While, if the dynamic safety distance adjustment mechanism is adopted, the collision probability under different v_r can be kept below 0.3%, which is far lower than the collision probability of a fixed safety distance. On the one hand, the dynamic safety distance adjustment mechanism

can avoid setting d_0 too small, which results in a large collision probability of vehicles. On the other hand, the dynamic safety distance adjustment mechanism can avoid setting d_0 too large, which results in a too-far safety distance between two vehicles, leading to a rear-end accident easily. Therefore, the dynamic safety distance adjustment mechanism can ensure the reliability and robustness of the AEB system and improve road traffic efficiency.

6 Conclusions

Various uncertainties exist in the autonomous driving system, such as the measurement errors of the sensors and the execution errors of the execution systems, which lead to the SOTIF problems of the autonomous driving system. This paper proposed a design method for autonomous driving systems with uncertainties. It took the AEB system as an example to introduce the design and optimization of the system with uncertainties in detail. Firstly, based on the AEB system model under the typical working scenario, the stochastic model with uncertainty parameters of the AEB system was established. For the multi-factor and multi-level characteristics of the AEB stochastic system, BBD schemes were adopted, and the MCS method was taken to obtain a large amount of data to establish the variance and distribution width surrogate models of the actual safety distance. Based on the variance surrogate model, the sensitivity of parameters to the system response was analyzed and the main parameters affecting the system performance were found. The influence of main uncertainty parameter combinations on the system performance was analyzed by potentiometric maps, and the combination of uncertainty parameters with minimum variance was found, which provided some references for the balance of performance and cost for the AEB system. Based on the distributed width surrogate model, a dynamic safety distance adjustment mechanism was established. Compared with the fixed safety distance, the dynamic safety distance can ensure the extremely low collision probability of the AEB system in various scenarios, which improved the reliability of the AEB system model under uncertainty and reduces the SOTIF problems of the AEB system.

This work provides a foundation for further research into the impact of the sensor precision decline caused by the aging of the sensor system or the disturbances in extreme weather on the autonomous driving system. Additionally, it offers insights into the adjustment strategy of the corresponding control parameters, thus, ensuring the maximum level of robustness and reliability of the autonomous driving system.

Acknowledgements The authors would like to appreciate the financial support of the Key Research and Development Projects of Anhui Province (Grant No. 202304a05020087), the Fundamental Research Funds for the Central Universities (Grant No. JZ2023YQTD0073) and the Innovation Project of New Energy Vehicle and Intelligent Connected Vehicle of Anhui Province (Grant No. JZ2021AFKJ00002).

Declarations

Conflict of interest On behalf of all the authors, the corresponding author states that there is no conflict of interest.

References

1. Peng, L., Wang, H., Li, J.: Uncertainty evaluation of object detection algorithms for autonomous vehicles. Auton. Innov. **4**(3), 12 (2021)
2. NHTSA: Collision Between a Car Operating with Automated Vehicle Control Systems and a Tractor-Semitrailer Truck Near Williston, Florida, May 7, 2016 (2016)
3. Guo, J., Kurup, U., Shah, M.: Is it safe to drive? An overview of factors, metrics, and datasets for driveability assessment in autonomous driving. IEEE Trans. Intell. Transp. Syst. **21**(8), 3135–3151 (2020)
4. Nilsson, J., Ali, M.: Sensitivity analysis and tuning for active safety systems. In: 13th International IEEE Conference on Intelligent Transportation Systems, pp. 161–167 (2010)
5. Zheng, P.J., McDonald, M.: The effect of sensor errors on the performance of collision warning systems. In: Proceedings of the 2003 IEEE International Conference on Intelligent Transportation Systems, pp. 469–474 (2003)
6. Dirndorfer, T., Botsch, M., Knoll, A.: Model-based analysis of sensor-noise in predictive passive safety algorithms. In: Proceedings of the 22nd Enhanced Safety of Vehicles Conference (2011)
7. Zang, S., Ding, M., Smith, D., et al.: The impact of adverse weather conditions on autonomous vehicles: how rain, snow, fog, and hail affect the performance of a self-driving car. IEEE Veh. Technol. Mag. **14**(2), 103–111 (2019)
8. Funfschilling, C., Perrin, G.: Uncertainty quantification in vehicle dynamics. Veh. Syst. Dyn. **57**(7), 1062–1086 (2019)
9. Kwon, K., Ryu, N., Seo, M., et al.: Efficient uncertainty quantification for integrated performance of complex vehicle system. Mech. Syst. Signal Process. **139**, 106601 (2020)
10. Stellet, J.E., Schumacher, J., Branz, W., et al.: Uncertainty propagation in criticality measures for driver assistance. In: 2015 IEEE Intelligent Vehicles Symposium (IV), pp. 1187–1194 (2015)
11. Stöckle, C., Utschick, W., Herrmann, S., et al.: Robust design of an automatic emergency braking system considering sensor measurement errors. In: Paper Presented at the 21st International Conference on Intelligent Transportation Systems (ITSC), Maui, HI, 2018–2023 Nov. 2018
12. Stöckle, C., Herrmann, S., Dirndorfer, T., et al.: Automated vehicular safety systems: robust function and sensor design. IEEE Signal Process. **37**(4), 24–33 (2020)
13. Stöckle, C., Utschick, W., Herrmann, S., et al.: Robust function and sensor design considering sensor measurement errors applied to automatic emergency braking. In: 2019 IEEE Intelligent Vehicles Symposium (IV), pp. 2284–2290 (2019)
14. Leyrer, M.L., Stöckle, C., Herrmann, S., et al.: An efficient approach to simulation-based robust function and sensor design applied to an automatic emergency braking system. In: 2020 IEEE Intelligent Vehicles Symposium (IV), pp. 617–622 (2020)

15. Lin, K.F., Stöckle, C., Herrmann, S., et al.: Robust function and sensor design considering sensor measurement errors applied to automatic emergency steering. In: 2020 IEEE Intelligent Vehicles Symposium (IV), pp. 610–616 (2020)
16. Macfarlane, J.F., Stroila, M.: Addressing the uncertainties in autonomous driving. SIGSPATIAL Spec. (2016). https://doi.org/10.1145/3024087.3024092
17. Zhu, Q., Li, W., Kim, H., et al.: Know the unknowns: addressing disturbances and uncertainties in autonomous systems. In: Paper Presented at ICCAD'20: IEEE/ACM International Conference on Computer-Aided Design, ACM (2020)
18. Roy, C.J., Oberkampf, W.L.: A comprehensive framework for verification, validation, and uncertainty quantification in scientific computing. Comput. Methods Appl. Mech. Eng. **200**(25), 2131–2144 (2011)
19. Zhang, T., Chen, X., Yu, Z., et al.: A Monte Carlo simulation approach to evaluate service capacities of EV charging and battery swapping stations. IEEE Trans. Ind. Inform. **14**(9), 3914–3923 (2018)
20. Zhang, W., Liang, Z., Wu, W., et al.: Design and optimization of a hybrid battery thermal management system for electric vehicle based on surrogate model. Int. J. Heat Mass Transf. **174**, 121318 (2021)
21. Li, X., et al.: Research on millimeter wave radar simulation model for intelligent vehicle. Int. J. Autom. Technol. **21**(2), 275–284 (2020)
22. Han, K., Lee, B., Choi, S.B.: Development of an antilock brake system for electric vehicles without wheel slip and road friction information. IEEE Trans. Veh. Technol. **68**(6), 5506–5517 (2019)
23. Rafiee, V., Faiz, J.: Robust design of an outer rotor permanent magnet motor through six-sigma methodology using response surface surrogate model. IEEE Trans. Magn. **55**(10), 1–10 (2019)
24. Jiang, Q., Zhou, P., Shao, X.: Verification methods for surrogate models. In: Jiang, Q., Zhou, P., Shao, X. (eds.) Surrogate Model-Based Engineering Design and Optimization, pp. 89–113. Springer, Singapore (2020)
25. Arun, V.V.: Multi-response optimization of artemia hatching process using split-split-plot design based response surface methodology. Sci. Rep. **7**(1), 40394 (2017)
26. Žuraulis, V., Garbinčius, G., Skačkauskas, P.: Experimental study of winter tyre usage according to tread depth and temperature in vehicle braking performance. Iran. J. Sci. Technol. Trans. Mech. Eng. **44**(1), 83–91 (2020)
27. Zhou, J., Du, Z., Yang, Z., et al.: Dynamic parameters optimization of straddle-type monorail vehicles based multiobjective collaborative optimization algorithm. Veh. Syst. Dyn. **58**(3), 357–376 (2020)